Flow Characteristics of Thermo-Responsive Microspheres in Microchannel during the Phase Transition

Ming-Yu Zhou, Rui Xie, Xiao-Jie Ju, Ze-Lin Zhao, and Liang-Yin Chu
School of Chemical Engineering, Sichuan University, Chengdu, Sichuan 610065, China

DOI 10.1002/aic.11769
Published online April 27, 2009 in Wiley InterScience (www.interscience.wiley.com).

*To probe into the flow and aggregation behaviors of thermo-responsive microspheres in microchannel during the phase transition, the flow characteristics of monodisperse poly(*n*-isopropylacrylamide) (PNIPAM) microspheres in microchannel with local heating are investigated systematically. When the fluid temperature in the microchannel increases across the lower critical solution temperature (LCST), the PNIPAM microspheres finish the phase transition within 10 s and are easily get aggregated during the phase transition. The diameter ratio of microsphere to microchannel, number of microspheres, initial distance between microspheres, and flow direction of fluid in microchannel, are key parameters affecting the flow and aggregation behaviors of the microspheres in microchannel during the phase transition. If a proper combination of these parameters is designed, the microspheres can aggregate together during the phase transition and stop automatically at a desired position in the microchannel by local heating, which is what the targeting drug delivery system expected.* © 2009 American Institute of Chemical Engineers *AIChE J,* 55: 1559–1568, 2009

*Keywords: microspheres, flow characteristics, poly(*n*-isopropylacrylamide), phase transition, aggregation*

Introduction

In recent years, environmental stimuli-responsive microspheres have attracted widespread interest from both scientific and technological aspects, because they may find many applications in the fields of controlled drug delivery,[1–4] chemical separation,[5–8] enzyme immobilization,[9,10] catalysis,[11] sensor[12,13] and so on. Such microspheres are able to change their physical–chemical properties and colloidal properties in response to fluctuations in environmental conditions, alone or in combination, including temperature,[14–21] pH,[22–25] magnetic field[26,27] and other stimuli signals.[28,29] There are many cases where environmental temperature fluctuations occur naturally, and in which the environmental temperature stimuli can be easily designed and artificially controlled. Therefore, much attention has been focused on thermo-responsive microspheres recently.

Most of previous researches on the thermo-responsive microspheres were focused on improving their monodispersity,[18] thermo-responsiveness[30–32] and controlled-release property.[33–35] Nevertheless, investigations on the flow characteristics of such microspheres during the phase transition are very few. The reason may exist in that such investigations fall into an interdisciplinary field, which might be easily to be neglected. To the best of our knowledge, only one paper from our group has reported investigations on the flow and aggregation behaviors of thermo-responsive millimeter-scale spheres in a transparent Pyrex glass pipe with 6.4 mm inner diameter[36]; whereas, prior reports on similar investigation in microchannel have not been found yet. However, if the thermo-responsive microspheres are applied to targeting drug delivery systems, their flow characteristics during the

Correspondence concerning this article should be addressed to L.-Y. Chu at chuly@scu.edu.cn

phase transition may directly affect the site-specific targeting performance. Besides, it is well known that the inner diameters of many blood vessels in human body fall in the range of hundreds of microns. Therefore, it is essential and very important to understand the flow characteristics of thermo-responsive microspheres in microchannel during the phase transition process.

The object of this study is to probe into flow characteristics of thermo-responsive microspheres during their phase transition in microchannel. Herein, the flow and aggregation behaviors of monodisperse poly(*N*-isopropylacrylamide) (PNIPAM) microspheres in glass capillary microchannel during their phase transition triggered by local heating are systematically investigated for the first time. The monodisperse PNIPAM microspheres are prepared by using a simple microfluidic device.[37] Thermo-responsive volume phase transition characteristics of the PNIPAM microspheres are investigated via measuring the temperature-dependent volume variation. The flow and aggregation behaviors of the monodisperse PNIPAM microspheres in the microchannel are recorded by a digital pickup camera equipped on an optical microscope. Influence parameters on the flow and aggregation behaviors of microspheres, such as the diameter ratio of microsphere to microchannel, number of microspheres, initial distance between microspheres, Reynolds number of fluid in microchannel, and flow direction of fluid in microchannel, are investigated systematically.

Experimental

Materials

NIPAM is kindly provided by Kohjin, Japan, and is used after recrystallization three times in hexane and acetone. *N*,*N*′-Methylene-bis-acrylamide (MBA) and ammonium persulfate (APS) are purchased from Chengdu Kelong Chemicals, China. Tetramethylethylenediamine (TEMED) is purchased from Tianhua Chemicals, China. Kerosene and sodium dodecyl sulfate (SDS) are purchased from Chengdu Sitong Chemicals, China. Polyglycerol polyricinoleate (PGPR 90) is purchased from Danisco, Denmark.

Synthesis of microspheres in a simple microfluidic device

Monodisperse PNIPAM microspheres are prepared using a simple microfluidic device (Figure 1). The dispersed phase is de-ionized water containing [NIPAM, 11.3% (w/v)], [MBA, 0.154% (w/v)], and [APS, 0.2% (w/v)]. The continuous phase is kerosene containing [PGPR 90, 14.125% (w/v)] and [TEMED, 3.5% (v/v)]. The dispersed and continuous phase solutions are pumped into the simple microfluidic device with adjustable flowrates by syringe pumps. The continuous phase flows through poly(vinyl chloride) (PVC) tubing (1 mm inner diameter and 3 mm outer diameter), and the dispersed phase is pumped into the PVC tubing via a 30-gauge needle (150 μm inner diameter) inserted through the wall of the PVC tubing with the needle tip located in the middle of the channel. The aqueous phase breaks into droplets at the tip of the needle, and the resultant droplets are carried away by the continuous phase flow, forming monodisperse W/O emulsion drops in the tubing. TEMED is both oil- and water-soluble; therefore, it can diffuse from kerosene to the emulsified aqueous phase and initiate the radical polymerization at room temperature. The PVC tubing with a length of 12 m ensures the complete polymerization of microspheres in the tube. The PNIPAM microspheres with different diameters are prepared at different flowrates of dispersed phase (4 ml/h and 2 ml/h, respectively), while at the same flowrate of continuous phase (120 ml/h).

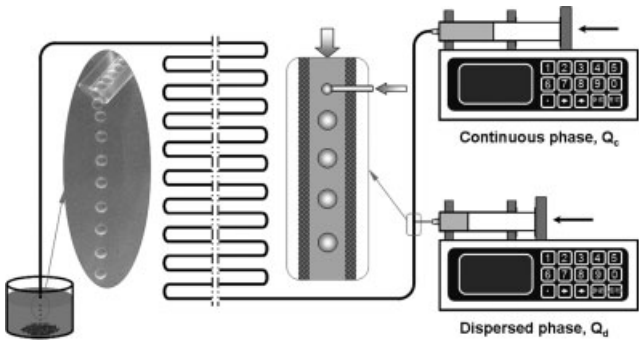

Figure 1. Schematic illustration of the simple microfluidic device for preparation of monodisperse PNIPAM microspheres.

Continuous phase is kerosene containing PGPR 90 and TEMED, and dispersed phase is de-ionized water containing NIPAM, MBA, and APS.

Measurement of thermo-responsive volume change characteristics of monodisperse PNIPAM microspheres

Thermo-responsive volume change characteristics of the prepared microspheres are studied by an optical microscope (BX 61, Olympus, Japan) equipped with a thermostatic stage system (TS 62, Instec) and a charge coupled device (CCD) camera. During the measurement, monodisperse PNIPAM microspheres are immersed in de-ionized water or SDS solution and the surrounding solution temperature is changed from 25 to 46°C via the thermostatic stage system. The diameters of microspheres are measured every 3°C, and the microsphere volumes as function of temperature are calculated. The volume change ratio, V_T/V_{46}, is defined as the ratio of the volume of microspheres at every examined temperature to that at 46°C.

Investigation of flow characteristics of PNIPAM microspheres in microchannel during the phase transition

The microchannel device (Figure 2a) with the function of local heat exchange is prepared using polymethyl methacrylate (PMMA) and glass capillary. In the observation section, the temperature range is designed to across the lower critical solution temperature (LCST) of PNIPAM microspheres in SDS solution. Before the experiments on flow behaviors, temperature distribution of the observation section along the testing microchannel is measured by utilizing an infrared thermo detector (MiniTemp MT6, Raytek) (Figure 2b). The temperature measurement errors are in control of $\pm$ 1°C. The interior diameter of the capillary is 520 μm, and the length of observation section is about 46 mm. To not only avoid the slack movement of PNIPAM microspheres but

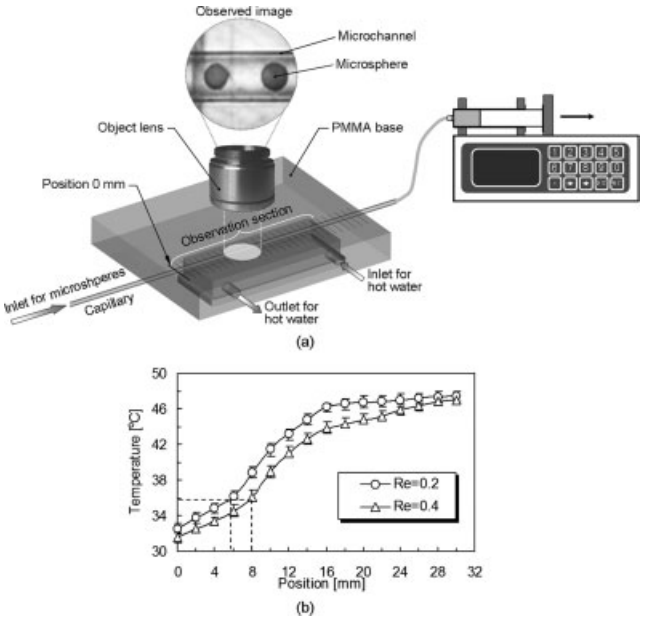

Figure 2. (a) Schematic illustration of experiment apparatus for investigating flow characteristics of PNIPAM microspheres and (b) the temperature distribution along the observation section of the microchannel at different Reynolds numbers.

also prevent the LCST of PNIPAM microspheres from changing a lot, 0.02 wt % SDS solution is introduced into the microchannel as the fluid. The average velocity of the fluid is obtained by dividing the flowrate of fluid by cross-section area of capillary. The flow and aggregation behaviors of PNIPAM microspheres during the phase transition are observed by an optical microscope (xs-212, JNOEC, China) from top, and a digital pickup camera (DSC-P50, SONY, Japan) equipped on the microscope is used to record the video. The average velocities of PNIPAM microspheres in the microchannel are calculated through the moving distance and relevant time interval. A series of corresponding optical micrographs are snatched by Windows Movie Maker from the videos to analyze the flow behaviors of PNIPAM microspheres. For measuring the velocity of microspheres, three to five parallel measurements are carried out to verify the repeatability, and the average data are used to plot the velocity figures.

Results and Discussion

Thermo-responsive volume phase transition characteristics of PNIPAM microspheres

Monodisperse PNIPAM microspheres are successfully prepared using the simple microfluidic device (Figure 1). The sizes of prepared PNIPAM microspheres are uniform (Figures 3a–c). To estimate the monodispersity of prepared PNIPAM microspheres, a parameter called coefficient of variation (*CV*) is introduced. *CV* is defined as the ratio of the standard deviation of size distribution to its arithmetic mean. The smaller the *CV* value is, the better the monodispersity of microspheres. The *CV* value of the prepared PNIPAM microspheres in de-ionized water at 25°C is 2.3%, indicating that the microspheres are highly monodisperse.

PNIPAM microspheres easily adhere to the inner wall of glass capillary, which results in a slack movement. To avoid such slack movement of PNIPAM microspheres during the observation of flow characteristics, SDS is added into the de-ionized water. Generally, silica and silicate glass surfaces immersed in water are known to acquire a negative surface charge density, primarily through the dissociation of terminal silanol groups.[38] On the other hand, high surface energy of microscale particles makes them easily adhere to other surfaces, so the PNIPAM particles can deposit onto glass surface easily. In the case, electrostatic charge of glass surface also plays an important role. As an anionic surfactant, SDS is able to adjust the surface charge and decrease the interfacial energy so as to reduce the possibility of particle deposition onto glass surface. Therefore, it makes the PNIPAM microspheres move swimmingly in the microchannel. The volume phase transition behavior of thermo-responsive PNIPAM microspheres is observed in both de-ionized water and SDS solution (Figure 3d). The maximal volume change ratio V_{25}/V_{46} (the ratio of volume at 25°C to that at 46°C) of PNIPAM microspheres in de-ionized water is about 16, and the LCST is about 32.2°C; while the maximal volume change ratio and the LCST of PNIPAM microspheres increases to about 22 and 35.7°C in 0.02 wt % SDS solution, respectively. At 25°C, the size of the same microspheres in 0.02 wt % SDS solution is larger than that in de-ionized water (Figures 3a, b, and d). As a kind of anionic surfactant, SDS molecules binds to the polymer network of PNIPAM microspheres through hydrophobic interactions, and subsequently converts a neutral PNIPAM hydrogel into a polyelectrolyte hydrogel. These acquired network charges and counterions associated to the charges exert an extra osmotic pressure on the network.[39] Therefore, the size and the LCST of PNIPAM microspheres increases. To observe the flow behaviors of microspheres more clearly, the prepared

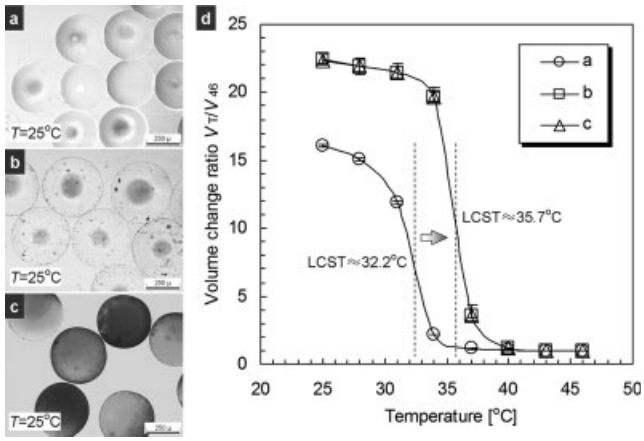

Figure 3. Optical micrographs (a-c) and thermo-responsive volume phase transition characteristics (d) of PNIPAM microspheres.

(a) Microspheres in de-ionized water, (b) microspheres in 0.02 wt % SDS solution, and (c) microspheres in 0.02 wt % SDS solution after dyeing in 0.05 wt % fuchsine solution. V_T and V_{46} are the microsphere volumes at T°C and 46°C, respectively.

PNIPAM microspheres are dyed into red by fuchsine (Figure 3c), and the experimental results show that fuchsine have no influence on both the maximal volume change ratio and the LCST of dyed PNIPAM microspheres (Figure 3d).

Flow characteristics of PNIPAM microspheres in horizontal microchannel at low Reynolds number of fluid

Flow behaviors of thermo-responsive PNIPAM microspheres are investigated using a self-made capillary microchannel device (inner diameter: 520 μm) (Figure 2a). Temperature distribution of the observation section along the testing microchannel is displayed in Figure 2b. The Reynolds numbers of fluid are tested to ensure the range of Reynolds number of fluid flow in the microchannel fall in laminar flow, since the character of blood flow is viscous laminar flow in microcirculation system.[40] Many interesting phenomena about the flow behaviors of PNIPAM microspheres with $d_s/D_{mc} = 0.913$ (where d_s stands for the diameter of PNIPAM microspheres and D_{mc} stands for the inner diameter of the microchannel) are found during the phase transition.

For one PNIPAM microsphere (Figure 4a), the process of phase transition is obviously observed along the microchannel when the fluid temperature increases across the LCST of PNIPAM microsphere in 0.02 wt % SDS solution. As is known, PNIPAM has both isopropyl (hydrophobic) and amidogen (hydrophilic) groups, and PNIPAM hydrogels can deswell or shrink as the environmental temperature increases from below the LCST to above the LCST and swell or expand as the temperature decreases from above the LCST to below the LCST.[36] When the microsphere comes to the position scale of 8 mm ($T = 35.7$°C), the environmental temperature equals to the LCST of PNIPAM ($T \approx 35.7$°C), so the whole polymer network starts to shrink, and the diameter of the microsphere starts to decrease from this position, and then decreases rapidly as the temperature continues increasing. The response time of the PNIPAM microsphere for the phase transition process is less than 10 s. Before the phase transition, the microsphere moves forward steadily with a constant velocity, and afterwards the velocity of microsphere keeps increasing during the phase transition, and then decreases after the phase transition (Figure 4b). Before the phase transition, as the microsphere is in the force balance (Figure 4c), it moves forward steadily with a constant velocity because of no acceleration. During the phase transition, the microsphere shrinks dramatically and rapidly, the liquid inside PNIPAM polymer network is squeezed out rapidly due to the large volume change ratio (about 22). As a result, a water layer forms around the microsphere, which removes the friction force (f) between the microsphere and the inner wall of capillary. Therefore, the force balance is broken, and an acceleration generates due to the drag force (F). Thus, the microsphere speeds up during this period. However, after the phase transition (i.e., the process of prompt deswelling finishes), the water layer surrounding the microsphere disappears, and the gravity (G) of the microsphere is larger than the buoyancy force (F''_b) after the phase transition. Hence, the microsphere locates in the bottom of the microchannel, where the local velocity is lower than the average velocity of the fluid. In addition, the

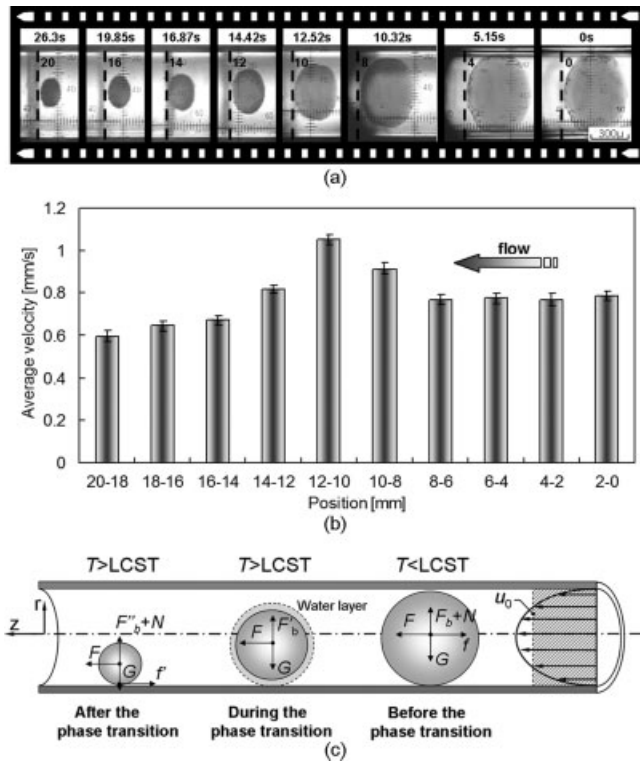

Figure 4. Flow characteristics of a PNIPAM microsphere ($d_s/D_{mc} = 0.913$) during the process of phase transition in horizontal microchannel. The Reynolds number of fluid is 0.4.

(a) Optical micrograph time series showing the movement of a PNIPAM microsphere during the phase transition process. The dashed line in the pictures is the position scale and the number near the dashed line is the position (unit: mm), (b) The average velocity distribution of the microsphere varied with position, (c) Forces acted on a PNIPAM microsphere in horizontal microchannel during the phase transition ($T >$ LCST) and after the phase transition ($T >$ LCST). u_0, F, N, and G are the average velocity of fluid, the drag force, the supporting force from the microchannel inner wall and gravity force respectively. f and f' are the friction forces before the phase transition and after the phase transition. F_b, F'_b and F''_b are the buoyancy forces before the phase transition, during the phase transition and after the phase transition respectively.

existence of friction force (f') also prevents the microsphere from moving forward. Therefore, the microsphere after the phase transition slows down.

For two PNIPAM microspheres, two situations are investigated as follows: one is that there is no initial distance between two microspheres (Figure 5a) at the entrance of observation section (position scale of 0 mm shown in Figure 2a), and the other is that the initial distance is 140 μm (Figure 6a). In the first situation, two microspheres move forward steadily one after the other at the beginning. When they come to the position scale of about 6 mm at which the temperature is 36.2°C, the temperature is above the LCST of PNIPAM, so the whole polymer networks of PNIPAM microspheres shrink dramatically, and the sphere diameters decrease dramatically and the velocities slow down. When they come to the position scale of 10 mm ($T = 41.5$°C), the deswelling process of PNIPAM microspheres has almost

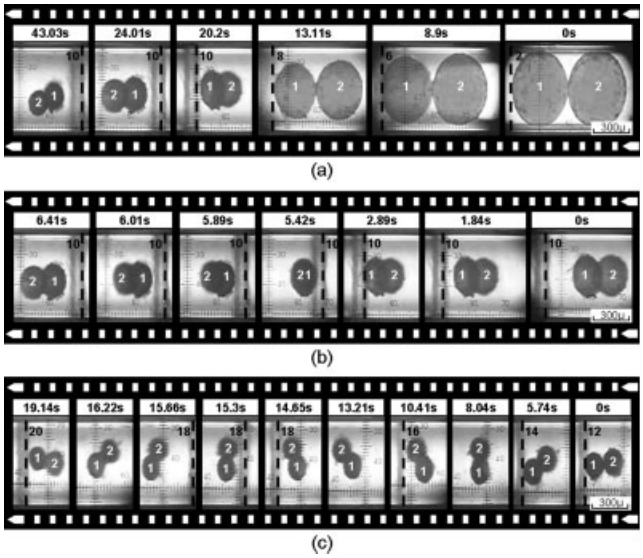

Figure 5. (a) Flow and aggregation characteristics of two PNIPAM microspheres (d_s/D_{mc} = 0.913) with initial distance of 0 μm during the process of phase transition in horizontal microchannel, (b) Overturn movement, and (c) swing movement of two aggregated microspheres after the phase transition.

All figures are observed from top. The Reynolds number of fluid is 0.2.

finished, since the interval time for the microspheres moving from position scale 6 mm to 10 mm (about 11.3 s) is longer than the phase transition time (less than 10 s). Thus, the surface of PNIPAM microsphere turns to hydrophobic. Because of the hydrophobic interaction of the surface of PNIPAM microspheres at high temperature ($T >$ LCST), the two microspheres aggregate together, and they start to overturn (Figure 5a). After the phase transition, two aggregated microspheres may roll forward (Figure 5b) or swing forward (Figure 5c) randomly.

When the initial distance between two PNIPAM microspheres is 140 μm (Figure 6a) at the entrance of observation section, the two microspheres move forward with the distance maintained as 140 μm at first. However, during the phase transition, with the temperature increasing, the surface distance between them becomes farther at first and then becomes closer, meanwhile the center distance decreases all along during the phase transition, and finally the microspheres aggregate together. From position scale 6 mm (T = 34.5°C) to 10 mm (T = 39°C), the temperature increases across the LCST of PNIPAM microspheres in 0.02 wt % SDS solution. Because temperature difference between two microspheres with initial distance of 140 μm could be neglected (Figure 3b), the phase transitions of the two microspheres occur almost isochronously. As a result, there is no difference of velocities between the two microspheres during this period (Figure 6b). Therefore, the central distance (d) between the centers of two microspheres does not change. However, when the microspheres flow toward downstream, the sizes of two microspheres decrease, consequently the surface distance (d_2) between the two microspheres increases (it seems that the distance of the two microspheres becomes longer) (Figures 6a and c). When the microspheres flow further toward downstream, the center distance decreases and the surface distance until two PNIPAM microspheres aggregate together. Even when the initial distance of two microspheres at the entrance of the observation section is as far as about 1000 μm, the microspheres can still get aggregated during the phase transition (Relevant pictures are not shown in this paper, because the eyeshot of microscope is too narrow to catch the two microspheres with such a far distance in the same view picture). The anterior microsphere always shrinks and slows down earlier than the posterior one and the distance between two microspheres decreases continuously till zero. Since the aggregation of the microspheres makes the contact area between the microspheres and the

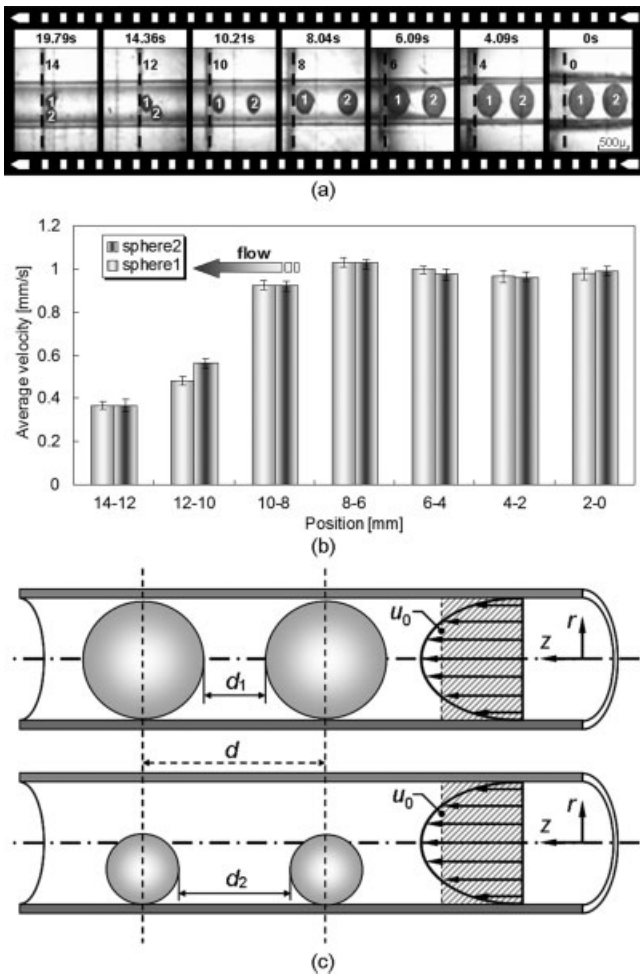

Figure 6. Flow characteristics of two PNIPAM microspheres (d_s/D_{mc} = 0.913) with initial distance of 140 μm during the process of phase transition in horizontal microchannel. The Reynolds number of fluid is 0.4.

(a) Optical micrograph time series showing the movement of two PNIPAM microspheres in the microchannel, (b) The average velocity distribution of two microspheres varied with position, (c) Distance variation between two microspheres during the phase transition. d and d_1 are the distances between the centers and between the surfaces of two microspheres before phase transition respectively, and d_2 is the distance between the surfaces of two microspheres after phase transition.

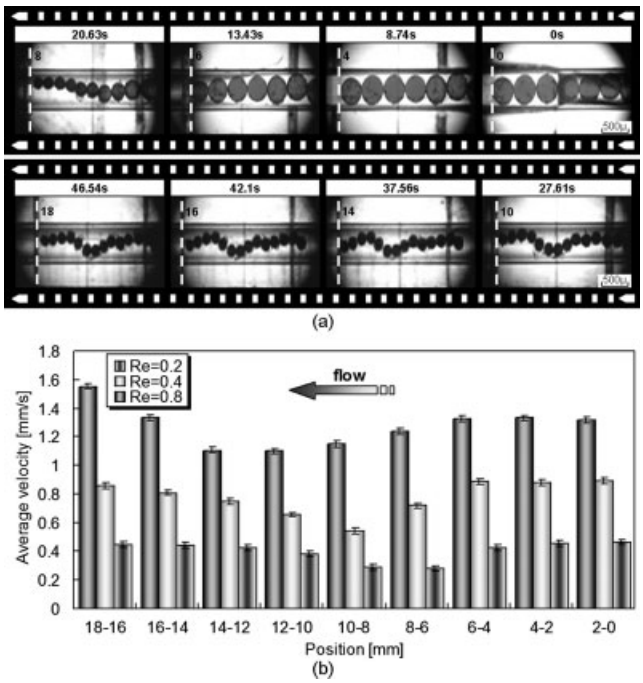

Figure 7. Flow and aggregation characteristics of 14 PNIPAM microspheres (d_s/D_{mc} = 0.913) during the process of phase transition in horizontal microchannel.

(a) Optical micrograph time series showing the movement of 14 PNIPAM microspheres in the microchannel. The Reynolds number of fluid is 0.2, (b) The average velocity distribution of microspheres varied with position at different Reynolds numbers of fluid.

inner wall of microchannel increase, the frictional resistance on the movement of microspheres increases. Therefore, the velocities of aggregated microspheres decrease more dramatically than that of a single microsphere during the phase transition. That is, the aggregation of PNIPAM microspheres makes them more easily to slow down or even stop at specific site when they suffer from local heating, which is what site-specific targeting drug delivery systems needed.

There are still some other factors that affect their site-specific targeting effectiveness in the microchannel. When the number of microspheres reaches 14 (Figure 7a), all of the microspheres aggregate together during the phase transition. When the phase transitions of anterior PNIPAM microspheres occur, their velocities decrease. The phase transitions of anterior microspheres occur before those of the posterior microspheres, as a result the posterior ones collide with the anterior ones and press them. Since the d_s/D_{mc} (i.e., 0.913) of the microspheres is too large, it is hard for the microspheres to overturn across one another in the microchannel. As a result, the microspheres can only move one by one and press each other, and the chain of aggregated PNIPAM microspheres transforms due to the definite flexibility, consequently the aggregated PNIPAM microspheres move forward with an "S" aggregation shape after the phase transition. For the 14 PNIPAM microspheres flowing in a line in the microchannel, when the phase transitions of anterior PNIPAM microspheres occur, their velocities decrease, which makes all the PNIPAM microspheres slow down during the phase transition. On the other hand, after the phase transition, the "S" aggregation shape can lead to the increase of effective area of fluid impetus. Therefore, unlike one or two microspheres, the aggregated 14 microspheres move faster rather than slow down after the phase transition (Figure 7b).

Effect of the diameter ratio of PNIPAM microsphere to microchannel on the flow characteristics

To investigate the effect of the diameter ratio of PNIPAM microsphere to microchannel on the flow characteristics, PNIPAM microspheres with d_s/D_{mc} = 0.596 are also prepared besides the aforementioned microspheres with d_s/D_{mc} = 0.913. For one PNIPAM microsphere with d_s/D_{mc} = 0.596 (Figure 8a), the process of phase transition in the microchannel is almost the same as that of one PNIPAM microsphere with d_s/D_{mc} = 0.913, but the velocity change during the phase transition is very different. Unlike the case of microspheres with d_s/D_{mc} = 0.913, the velocity of the PNIPAM microsphere with d_s/D_{mc} = 0.596 decreases during the phase transition instead of increasing, which is just similar to the velocity variation of millimeter-scale PNIPAM hydrogel sphere (d_s/D_{mc} = 0.608) during the phase transition.[36] Since the maximal volume change ratio (about 10 for PNIPAM microsphere with d_s/D_{mc} = 0.596 and 7 for millimeter-scale PNIPAM hydrogel sphere with d_s/D_{mc} = 0.608) is not so large that the effect of water layer surrounding the microsphere during the thermo-responsive phase transition is not so obvious during the phase transition. Compared with the PNIPAM microsphere with d_s/D_{mc} = 0.913, the velocity of microsphere in this study decreases to a much larger extent, and at last the microsphere even stops just after the phase transition (Figure 8). The microsphere with d_s/D_{mc} = 0.596 can shrink smaller than the microsphere with d_s/D_{mc} =

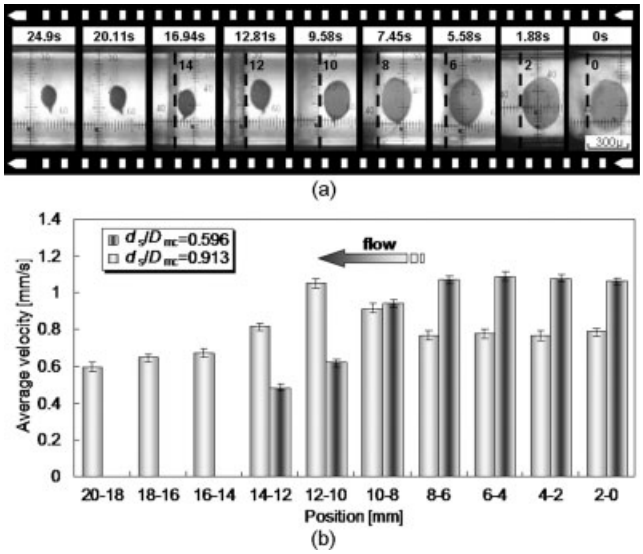

Figure 8. Flow characteristics of a PNIPAM microsphere (d_s/D_{mc} = 0.596) during the process of phase transition in horizontal microchannel.

(a) Optical micrograph time series showing the movement of a PNIPAM microsphere in the microchannel. The Reynolds number of fluid is 0.4, (b) The average velocity variation of microspheres with different ratios of d_s/D_{mc} along the position.

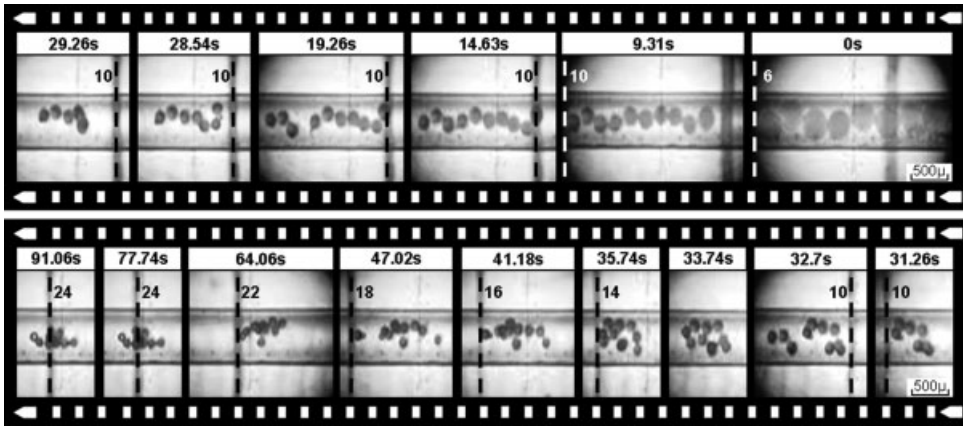

Figure 9. Flow and aggregation characteristics of 10 PNIPAM microspheres (d_s/D_{mc} = 0.596) during the process of phase transition in horizontal microchannel.

The Reynolds number of fluid is 0.2.

0.913 after the phase transition; on the other hand, the local velocity of fluid decreases from the central axis to the bottom of the microchannel. When the microsphere shrinks and comes to the bottom of the microchannel, the smaller the shrunken microsphere is, the lower the local velocity of fluid is. Therefore, the microsphere with smaller size (d_s/D_{mc} = 0.596) can slow down or even stop after the phase transition more easily than the bigger one (d_s/D_{mc} = 0.913).

When 10 PNIPAM microspheres with d_s/D_{mc} = 0.596 move along the microchannel (Figure 9), they also aggregate together during the phase transition. Unlike the aggregation of the larger microspheres with d_s/D_{mc} = 0.913 mentioned above (Figure 7a), the PNIPAM microspheres with d_s/D_{mc} = 0.596 can overturn across one another easily during the phase transition, and finally 10 PNIPAM microspheres aggregate to a large agglomerate. The aggregated microspheres stop at a certain position after the phase transition, which is almost the same as the phenomenon of 10 mm-scale PNIPAM hydrogel spheres (d_s/D_{mc} = 0.608).[36] The results indicate that the value of d_s/D_{mc} can determine the aggregation configuration of PNIPAM microspheres during the phase transition, and then the velocity change of the aggregated microspheres. That is, the value of d_s/D_{mc} is a key parameter affecting the flow characteristics of PNIPAM microspheres during the phase transition. Therefore, to design thermoresponsive targeting drug delivery systems, d_s/D_{mc} should be taken into account properly to achieve site-specific stop of microsphere carriers by local heating.

Effect of fluid flow direction on flow characteristics of PNIPAM microspheres

Considering the directional complexity of blood vessels in human body, flow characteristics of PNIPAM microspheres in vertical microchannels are also investigated in addition to that in horizontal microchannel. The fluid is designed to flow either from upside to downside or from downside to upside. For both one and 10 PNIPAM microspheres (Figure 10) moving from upside to downside in vertical microchannel, the velocity increases dramatically during the phase transition, which is definitely different from that in horizontal microchannel. Because the buoyancy force during the phase transition (F_b) is in direct proportion to the volume of the PNIPAM microsphere, the F_b decreases as the microsphere volume decreases. During the phase transition, when the sizes of microspheres decrease, the buoyancy force acting on the microspheres correspondingly decreases. On the other hand, because the gravity of the microsphere keeps constant, the resultant downward force acts on the microsphere increases, which leading to an increase in the velocity of microsphere in the vertical microchannel.

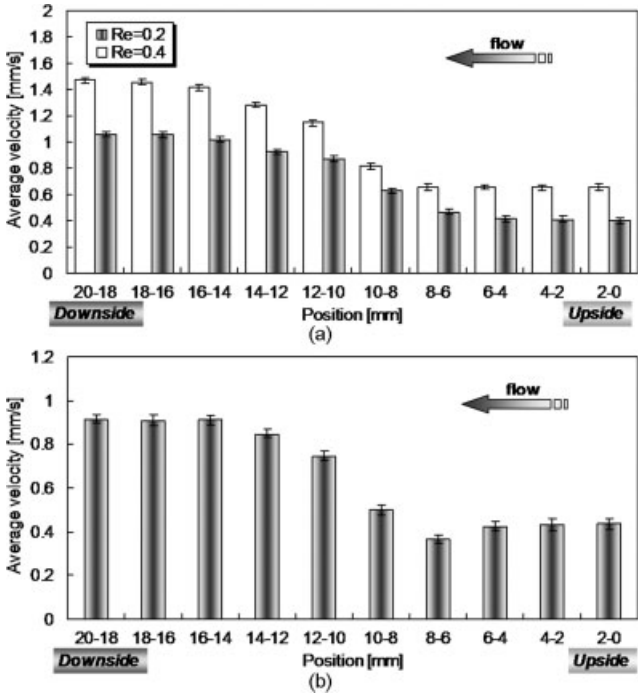

Figure 10. Velocity variations of a PNIPAM microsphere (d_s/D_{mc} = 0.913) (a) and 10 PNIPAM microspheres (d_s/D_{mc} = 0.913) with Reynolds number of 0.2 and (b) during the process of phase transition in vertical microchannel from upside to downside.

On the other hand, the phenomena are totally different when PNIPAM microspheres move from downside to upside in vertical microchannel. For one PNIPAM microsphere in vertical microchannel (Figure 11), the variation of velocity and the movement during the phase transition are similar to that in horizontal microchannel. Nevertheless, after the phase transition, the velocity of the microsphere decreases to a larger extent. Because F_b decreases as the microsphere diameter decreases, and the gravity of the microsphere keeps constant; therefore, the resultant upward force acts on the microsphere decreases, which results in a dramatic decrease in the velocity of microsphere. On the other hand, the movement of the microsphere after the phase transition is different from that of millimeter-scale hydrogel sphere in vertical pipe.[36] In millimeter-scale pipe, the hydrogel sphere moves upward along an "S" track after the phase transition because of the existence of Saffman force in the radial direction; however, there is no similar "S" track movement in the microchannel.

The calculation formula of Saffman force (F_L) has been given by Saffman as follows[41]:

$$F_L = KVa^2k^{\frac{1}{2}}/v^{\frac{1}{2}} \quad (1)$$

where, K is a constant coefficient and its value has been obtained by numerical integration as 81.2; V is the relative velocity of particle and fluid measured on the streamline through the centre; a is the radius of the particle; k is the velocity gradient and v is the kinematic viscosity. In the previous minichannel,[36] V, a, and k are 7.5 mm/s, 1.95 mm and 9.7 s^{-1} respectively. In the current microchannel, V, a, and k are 0.38 mm/s, 0.24 mm, and 3.3 s^{-1} respectively. Since only 0.02 wt % SDS is added into de-ionized water in this study, there is little difference between v values of de-ionized water and 0.02 wt % SDS solution. The calculated results show that the Saffman force in the previous minichannel is about 2257 times larger than the Saffman force in the current microchannel. Therefore, the Saffman force in this study is considered to be too weak to result in the "S" motion of microsphere in the microchannel.

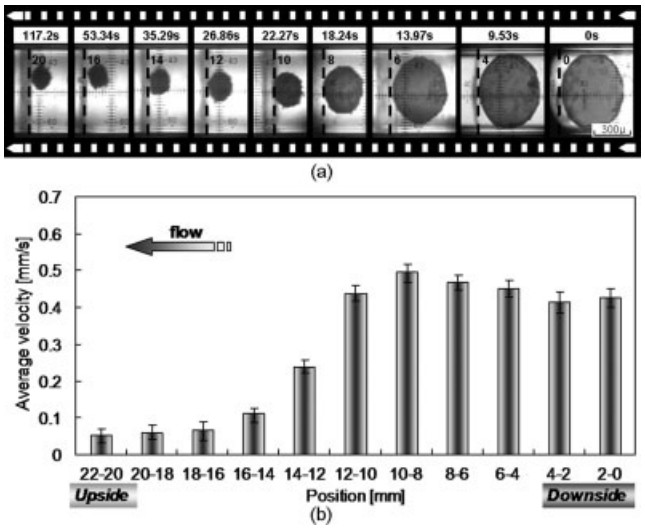

Figure 11. Flow characteristics of a PNIPAM microsphere (d_s/D_{mc} = 0.913) during the process of phase transition in vertical microchannel from downside to upside.

The Reynolds number of fluid is 0.2. (a) Optical micrograph time series showing the movement of a PNIPAM microsphere in the microchannel, (b) The average velocity variation of the microsphere along the position.

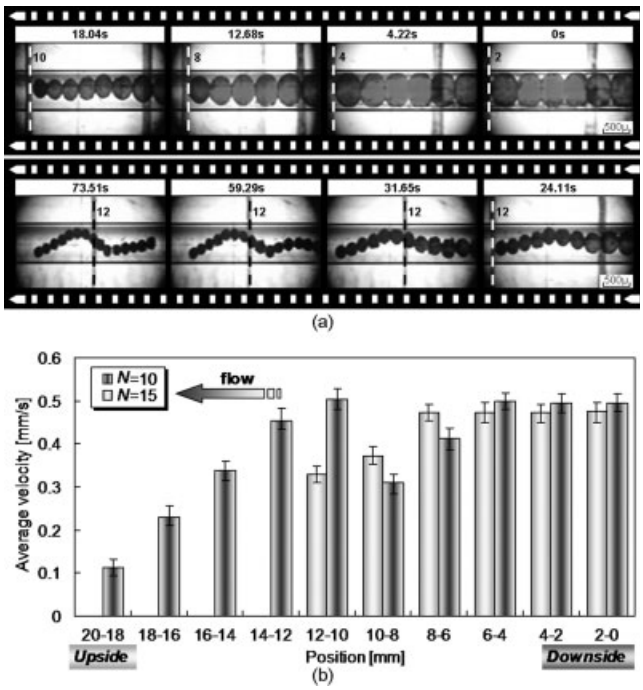

Figure 12. Flow and aggregation characteristics of 10 and 15 PNIPAM microspheres (d_s/D_{mc} = 0.913) during the process of phase transition in vertical microchannel from downside to upside.

The Reynolds number of fluid is 0.2. (a) Optical micrograph time series showing the movement of 15 PNIPAM microspheres in the microchannel, (b) The average velocity variation of 10 and 15 microspheres along the position.

If 10 PNIPAM microspheres move from downside to upside, they aggregate during the phase transition and their velocity decreases dramatically after the phase transition (Figure 12b). When the number of microspheres comes to 15, the aggregated microspheres stop at a certain position during the phase transition, mainly due to the decrease of buoyancy force (Figure 12a).

The flow direction of fluid in microchannel has great effect on site-specific targeting performance of PNIPAM microspheres during local heating. This gives us valuable information for designing site-specific targeting drug delivery systems in the future.

Conclusions

Flow characteristics of thermo-responsive PNIPAM microspheres during the phase transition in microchannels are investigated in this study for the first time. Monodisperse PNIPAM microspheres are prepared using a simple microfluidic device. These microspheres are monodispersed and featured with excellent thermo-responsive volume phase transition characteristics. The PNIPAM microspheres can respond to environment temperature quickly and the

response time is less than 10 s for the phase transition in the microchannel. Many interesting flow behaviors of the PNIPAM microspheres during the phase transition are found in microchannel. The velocity of one microsphere with $d_s/D_{mc} = 0.913$ in horizontal microchannel increases first during the phase transition and then decreases after the phase transition. The PNIPAM microspheres are easy to aggregate together in the microchannel during the phase transition, even if the initial distance between two PNIPAM microspheres at entrance of the observation section is as long as 1000 μm. When the microsphere diameter is smaller ($d_s/D_{mc} = 0.596$), the flow behaviors in the microchannel are different. In horizontal microchannels, 14 aggregated PNIPAM microspheres with $d_s/D_{mc} = 0.913$ speed up after the phase transition; however, 10 aggregated PNIPAM microspheres with $d_s/D_{mc} = 0.596$ stop at certain position after the phase transition. The aggregation configuration of PNIPAM microspheres is determined by the value of d_s/D_{mc}, which ultimately plays a crucial part in the velocity variation of PNIPAM microspheres during the phase transition. For designing thermo-responsive targeting drug delivery systems, it is very important to choose a proper value of d_s/D_{mc}. The flow direction of fluid in microchannel also has dramatic influence on the flow characteristics of PNIPAM microspheres during the phase transition. Compared with the velocity variation of microspheres move from upside to downside, definitely different phenomenon of velocity variation is observed when the microspheres move from downside to upside. The results in this study provide important information for future applications of PNIPAM microspheres in the therapeutical and biotechnological fields, especially in thermo-responsive site-specific targeting.

Acknowledgements

This work was supported by the National Natural Science Foundation of China (20674054), the Key Project of the Ministry of Education of China (106131), and Sichuan Youth Science and Technology Foundation for Distinguished Young Scholars (08ZQ026-042). The authors thank Kohjin Co., Ltd, Japan, for kindly supplying the *N*-isopropylacrylamide.

Literature Cited

1. Jeong B, Bae YH, Lee DS, Kim SW. Biodegradable block copolymers as injectable drug-delivery systems. *Nature*. 1997;388:860–862.
2. Ichikawa H, Fukumori Y. A novel positively thermosensitive controlled-release microcapsule with membrane of nano-sized poly(*N*-isopropylacrylamide) gel dispersed in ethylcellulose matrix. *J Control Release*. 2000;63:107–119.
3. Murthy N, Thng YX, Schuck S, Xu MC, Frechet JMJ. A novel strategy for encapsulation and release of proteins: Hydrogels and microgels with acid-labile acetal cross-linkers. *J Am Chem Soc*. 2002;124:12398–12399.
4. Wang XQ, Wenk E, Hu X, Castro GR, Meinel L, Wang XY, Li C, Merkle H, Kaplan DL. Silk coatings on PLGA and alginate microspheres for protein delivery. *Biomaterials*. 2007;28:4161–4169.
5. Arai F, Ng C, Maruyama H, Ichikawa A, EI-Shimy H, Fukuda T. On chip single-cell separation and immobilization using optical tweezers and thermosensitive hydrogel. *Lab Chip*. 2005;5:1399–1403.
6. Slomkowski S. Polyacrolein containing microspheres: synthesis, properties and possible medical applications. *Prog Polym Sci*. 1998;23:815–874.
7. Sun HH, Li XN, Ma GH, Su ZG. Polystyrene-type uniform porous microsphere enables high resolution and low-pressure chromatography of natural products—A case study with icariin purification. *Chromatographia*. 2005;61:9–15.
8. Jiang XY, Bai S, Sun Y. Fabrication and characterization of rigid magnetic monodisperse microspheres for protein adsorption. *J Chromatogr B*. 2007;852:62–68.
9. Guiseppi-Elie A, Sheppard NF, Brahim S, Narinesingh D. Enzyme microgels in packed-bed bioreactors with downstream amperometric detection using microfabricated interdigitated microsensor electrode arrays. *Biotechnol Bioeng*. 2001;75:475–484.
10. Phadtare S, Kumar A, Vinod VP, Dash C, Palaskar DV, Rao M, Shukla PG, Sivaram S, Sastry M. Direct assembly of gold nanoparticle "shells" on polyurethane microsphere "cores" and their application as enzyme immobilization templates. *Chem Mater*. 2003;15:1944–1949.
11. Li XZ, Liu H. Photocatalytic oxidation using a new catalyst—TiO_2 microsphere—for water and wastewater treatment. *Environ Sci Technol*. 2003;37:3989–3994.
12. Michael KL, Taylor LC, Schultz SL, Walt DR. Randomly ordered addressable high-density optical sensor arrays. *Anal Chem*. 1998;70:1242–1248.
13. Liu DF, Xiang YJ, Wu XC, Zhang ZX, Liu LF, Song L, Zhao XW, Luo SD, Ma WJ, Shen J, Zhou WY, Wang G, Wang CY, Xie SS. Periodic ZnO nanorod arrays defined by polystyrene microsphere self-assembled monolayers. *Nano Lett*. 2006;6:2375–2378.
14. Yoshida R, Uchida K, Kaneko Y, Sakai K, Kikuchi A, Sakurai Y, Okano T. Comb-type grafted hydrogels with rapid de-swelling response to temperature-changes. *Nature*. 1995;374:240–242.
15. Kondo A, Fukuda H. Preparation of thermo-sensitive magnetic microspheres and their application to bioprocesses. *Colloids Surf A*. 1999;153:435–438.
16. Xie XF, Fan XH. Synthesis of thermo-sensitive functional polymer microspheres using macromonomer poly(*N*-vinylformamide) and styrene. *Acta Polym Sin*. 2001;3:347–350.
17. Xiao XC, Chu LY, Chen WM, Wang S, Li Y. Positively thermosensitive monodisperse core-shell microspheres. *Adv Funct Mater*. 2003;13:847–852.
18. Xiao XC, Chu LY, Chen WM, Wang S, Xie R. Preparation of submicrometer-sized monodispersed thermoresponsive core-shell hydrogel microspheres. *Langmuir*. 2004;20:5247–5253.
19. Xiao XC, Chu LY, Chen WM, Zhu JH. Monodispersed thermoresponsive hydrogel microspheres with a volume phase transition driven by hydrogen bonding. *Polymer*. 2005;46:3199–3209.
20. Zhang Y, Ding JD. Preparation of thermo-sensitive polymer microgels by altered-temperature suspension polymerization. *Acta Polym Sin*. 2005;6:919–923.
21. Pich A, Tessier A, Boyko V, Lu Y, Adler HJP. Synthesis and characterization of poly(vinylcaprolactam)-based microgels exhibiting temperature and pH-sensitive properties. *Macromolecules*. 2006;39:7701–7707.
22. Kumar ABM, Rao KP. Preparation and characterization of pH-sensitive proteinoid microspheres for the oral delivery of methotrexate. *Biomaterials*. 1998;19:725–732.
23. Eichenbaum GM, Kiser PF, Simon SA, Needham D. pH and ion-triggered volume response of anionic hydrogel microspheres. *Macromolecules*. 1998;31:5084–5093.
24. Tan BH, Ravi P, Tam KC. Synthesis and characterization of novel pH-responsive polyampholyte microgels. *Macromol Rapid Commun*. 2006;27:522–528.
25. Hu L, Chu LY, Yang M, Wang HD, Niu CH. Preparation and characterization of novel cationic pH-responsive poly(*N*,*N*′-dimethylamino ethyl methacrylate) microgels. *J Colloid Interface Sci*. 2007;311:110–117.
26. Xiao A, Hu JH, Wang CC, Jiang DL. Synthesis of magnetic microspheres with controllable structure via polymerization-triggered self-positioning of nanocrystals. *Small*. 2007;3:1811–1817.
27. Toprak MS, Mckenna BJ, Mikhaylova M, Waite JH, Stucky GD. Spontaneous assembly of magnetic microspheres. *Adv Mater*. 2007;19:1362–1368.
28. Wang JF, Cormack PAG, Sherrington DC, Khoshdel E. Monodisperse, molecularly imprinted polymer microspheres prepared by precipitation polymerization for affinity separation applications. *Angew Chem Int Edit*. 2003;42:5336–5338.
29. Carter SR, Rimmer S. Molecular recognition of caffeine by shell molecular imprinted core-shell polymer particles in aqueous media. *Adv Mater*. 2002;14:667–670.

30. Lizawa T, Matsuura Y, Onohara Y. Synthesis of thermosensitive poly(*N*-alkylacrylamide) gels and core-shell type gels. *Polymer*. 2005;46:8098–8106.
31. Wei HL, Yu HQ, Zhang AY, Sun LG, Hou DD, Feng ZG. Synthesis and characterization of thermosensitive and supramolecular structured hydrogels. *Macromolecules*. 2005;38:8833–8839.
32. Zhang XZ, Chu CC. Fabrication and characterization of microgel-impregnated, thermosensitive PNIPAAm hydrogels. *Polymer*. 2005; 46:9664–9673.
33. Hsiue GH, Hsu SH, Yang CC, Lee SH, Yang IK. Preparation of controlled release ophthalmic drops, for glaucoma therapy using thermosensitive poly-*N*-isopropylacrylamide. *Biomaterials*. 2002;23:457–462.
34. Eeckman F, Moes AJ, Amighi K. Surfactant induced drug delivery based on the use of thermosensitive polymers. *J Control Release*. 2003;88:105–116.
35. Huang G, Gao J, Hu ZB, John JVS, Ponder BC, Moro D. Controlled drug release from hydrogel nanoparticle networks. *J Control Release*. 2004;94:303–311.
36. Zhou MY, Chu LY, Chen WM, Ju XJ. Flow and aggregation characteristics of thermo-responsive poly (*N*-isopropylacrylamide) spheres during the phase transition. *Chem Eng Sci*. 2006;61:6337–6347.
37. Quevedo E, Steinbacher J, McQuade DT. Interfacial polymerization within a simplified microfluidic device: capturing capsules. *J Am Chem Soc*. 2005;127:10498–10499.
38. Behrens SH, Grier DG. The charge of glass and silica surface. *J Chem Phys*. 2001;115:6716–6721.
39. Kokufuta E, Zhang YQ, Tanaka T, Mamada A. Effects of surfactants on the phase transition of poly(*N*-isopropylacrylamide) gel. *Macromolecules*. 1993;26:1053–1059.
40. Mairey E, Genovesio A, Donnadieu E, Bemard C, Jaubert F, Pinard E, Seylaz J, Olivo-Marin JC, Nassif X, Dumenil G. Cerebral microcirculation shear stress levels determine *Neisseria meningitidis* attachment sites along the blood-brain barrier. *J Exp Med*. 2006;203: 1939–1950.
41. Saffman PG. The lift on a small sphere in a slow shear flow. *J Fluid Mech*. 1965;22:385–400.

Manuscript received Feb. 29, 2008, revision received Aug. 4, 2008, and final revision received Nov. 21, 2008.